Acta Pharmacologica Sinica (2015) 36: 928–938
© 2015 CPS and SIMM All rights reserved 1671-4083/15
www.nature.com/aps

Original Article

Connexin 43 stabilizes astrocytes in a stroke-like milieu to facilitate neuronal recovery

Le-yu WU, Xue-li YU, Lin-yin FENG*

CAS Key Laboratory of Receptor Research, Shanghai Institute of Materia Medica, Chinese Academy of Sciences, Shanghai 201203, China

Aim: Connexin 43 (Cx43) is a member of connexin family mainly expressed in astrocytes, which forms gap junctions and hemichannels and maintains the normal shape and function of astrocytes. In this study we investigated the role of Cx43 in astrocytes in facilitating neuronal recovery during ischemic stroke.
Methods: Primary culture of astrocytes or a mixed culture of astrocytes and cortical neurons was subjected to oxygen glucose deprivation and reperfusion (OGD/R). The expression of Cx43 and Ephrin-A4 in astrocytes was detected using immunocytochemical staining and Western blot assays. Intercellular Ca^{2+} concentration was determined with Fluo-4 AM fluorescent staining. Middle cerebral artery occlusion (MCAO) model rats were used for *in vivo* studies.
Results: OGD/R treatment of cultured astrocytes caused a decrement of Cx43 expression and translocation of Cx43 from cell membrane to cytoplasm, accompanied by cell retraction. Furthermore, OGD/R increased intracellular Ca^{2+} concentration, activated CaMKII/CREB pathways and upregulated expression of Ephrin-A4 in the astrocytes. All these changes in OGD/R-treated astrocytes were alleviated by overexpression of Cx43. In the cortical neurons cultured with astrocytes, OGD/R inhibited the neurite growth, whereas overexpression of Cx43 or knockdown of Ephrin-A4 in astrocytes restored the neurite growth. In MCAO model rats, neuronal recovery was found to be correlated with the recuperation of Cx43 and Ephrin-A4 in astrocytes.
Conclusion: Cx43 can stabilize astrocytes and facilitate the resistance to the deleterious effects of a stroke-like milieu and promote neuronal recovery.

Keywords: astrocytes; Connexin 43; oxygen-glucose deprivation/recovery; middle cerebral artery occlusion; CREB; Ephrin-A4; calcium

Acta Pharmacologica Sinica (2015) 36: 928–938; doi: 10.1038/aps.2015.39; published online 22 June 2015

Introduction

Stroke is a hazardous cerebrovascular event with a high incidence rate. Ischemic stroke causes a rapid loss of brain function as a result of a disruption of the blood supply to the brain and has a higher incidence than hemorrhagic stroke. Currently, medication for strokes mainly focuses on neurons, and the glia and neuron-glia interactions are neglected, which could compromise the therapeutic effects of the treatment[1]. To discover novel targets, researchers have shifted to considering other non-neuronal cells and elucidating how they function in stroke progression.

Astrocytes are among these non-neuronal cells and are predominant in the central nervous system. After activation by a stroke and the related milieu, astrocytes are hostile to neuronal recovery. Primarily, astrocytes amplify neuroinflammation by secreting various types of cytokines and chemokines[2]. In addition, astrocytes can proliferate and form glial scars, which impedes the growth of neurons. The glial scar embodies the extracellular matrix and includes a plethora of components, such as chondroitin sulfate proteoglycans, Sema3A, fibronectin, and collagen[3, 4]. Among them, EphA4 has not been exculpated from inhibiting neuronal recovery. Evidence has shown that EphA4, expressed both in astrocytes and neurons, is detrimental to the growth of neurons. The binding of ligands (*ie*, Ephrin-A1, Ephrin-A3, Ephrin-A4, Ephrin-A5) is the premise for the inhibitory effect of EphA4. Moreover, it was found that Ephrin-A4 inhibited neurite growth in the peripheral nervous system[5].

Inhibiting and reversing the activation of astrocytes appears to be rational and practical. However, the complete progression of a stroke and neuronal recovery are extremely complicated. Specifically, inhibiting inflammation-related signaling pathways, which also exert essential functions in normal cells, to deactivate astrocytes is uneven. Therefore, it may be expe-

* To whom correspondence should be addressed.
E-mail lyfeng@simm.ac.cn
Received 2015-02-13 Accepted 2015-04-02

dient to stabilize astrocytes or appropriately return them to a normal state.

The functions of Cx43 in astrocytes should not be neglected in brain development, ischemia, neurodegenerative disease and brain injury. Astrocyte-restricted disruption of Cx43 could dampen neuronal plasticity in the barrel cortices of mice[6]. It has been reported that Cx43 could be protective by releasing ATP. Moreover, the inflammatory milieu could cause the opposite regulation of gap junctions and hemichannels[7–9], which are two types of functional units composed of Cx43. Functionally increased hemichannels by hypoxia or pro-inflammatory factors can mediate the release of deleterious substances that could impair glial and neuronal survival[7, 10]. While functional decrements in gap junctions disturb cell-cell communication and could disarm the buffering reservoir of astrocyte networks, rectifying the function of gap junctions might improve the rate of neuronal death[11]. Both glia and neurons could benefit from bone marrow stromal cells and human marrow stromal cells based on the recovery of Cx43 as well as the functional units composed of Cx43[12, 13]. Therefore, Cx43 could possibly be a basis or even a potential target for neuroprotection during ischemia or brain injury. Herein we utilized oxygen glucose deprivation/recovery (OGD/R) and middle cerebral artery occlusion (MCAO) to simulate ischemic stroke. It was found that Cx43 was significant for the integrity and stability of astrocytes. Ameliorating alterations of Cx43 could promote cell integrity and the stability of astrocytes treated with OGD/R, and the growth of cortical neurons could be sustained.

Materials and methods

Animals

All the male Sprague-Dawley (SD) rats were provided by SLAC Laboratory Animals Co Ltd (Shanghai, China). The use of animals and experimental procedures were performed following the rules of the Association for Assessment and Accreditation of Laboratory Animal Care International.

Primary culture of astrocytes and cortical neurons

A purified primary culture of astrocytes was derived from SD rats at postnatal d 1 (P0). After anaesthetization with an ice bath, rat pups were soaked in 75% ethanol, and their brains were dissected into separate cortices. Then, the separated cortices were minced and digested with 0.125% trypsin. The cell suspensions were grown in 75 cm^2 culturing flasks pre-coated with poly-D-lysine (Sigma, CAT# P0899) at a density of approximately 2×10^6 cells/mL. The cells were cultured in high glucose Dulbecco's modified Eagle'smedium(DMEM, Gibco, CAT# 12800-017) with 10% horse serum (Gibco, CAT# 16050-122) in an incubator (ThermoFisher Scientific, Waltham, MA, USA) with 5% CO_2 and 95% humid air at 37 °C. After seven days, the culture flasks were shaken in a rotatory shaker at 200 rounds/min for 8 h to remove neurons and oligodendrocytes. The remaining adhered cells were eliminated by cytosine arabinoside (final concentration 10 μmol/L) treatment. The purity of the astrocytes in the cultures was more than 98%, which was verified by immunocytochemistry staining utilizing anti-GFAP antibodies (Millipore, MAB360, 1:300). SD rat fetuses (E17) were utilized to obtain a primary culture of cortical neurons. Pregnant rats were anaesthetized with chloral hydrate at a dosage of 35 mg/100 g. Then, dissection was performed to collect the fetuses in uteruses. The collected fetuses were soaked in 4 °C pre-cold D-Hanks solution followed by the separation of brains and cortices under a stereoscopic microscope. The cortices were minced and digested with 0.125% trypsin for 10 min at 37 °C. After the digestion was terminated by DMEM with 10% FBS, cortices were suspended with a Pasteur pipette. Suspensions were collected to obtain cells via centrifugation. The cells were transfected with DsRed plasmids via an AMAXA Nucleofector kit. Then, they were plated at densities of 10^4/mL onto the astrocyte (with or without OGD/R treatment) culture.

OGD/R of astrocytes

First, the astrocyte primary culture medium was changed with DMEM without glucose and serum. The treatment of OGD was performed in a specially fabricated plexiglass chamber filled with a mixture of 95% N_2 and 5% CO_2 at 37 °C. After 6 h of OGD, astrocytes were cultured in high glucose DMEM with 10% FBS in an incubator with 5% CO_2 and 95% humid air at 37 °C, which simulated reperfusion of an ischemic stroke.

MCAO

Experimental procedures were basically consistent with methods reported earlier[14, 15]. Briefly, male SD rats that weighed 250–280 g were anesthetized with 45 mg/kg pentobarbital sodium. The left external carotid artery (ECA) was separated and ligated proximally to create a cross of Y-shaped carotid arteries. Nylon sutures were inserted into the internal carotid artery (ICA) via the common carotid artery (CCA) and fixed by a cotton suture tied around the ICA when the CCA was ligated distally in advance to block the middle cerebral artery (MCA). Then, the incision was sutured. The inserted nylon suture was pulled out after 1 h of ischemia to initiate reperfusion. The animals were euthanized at d 1 or d 8 after perfusion.

Overexpression of Cx43 and Ephrin-A4 RNAi

The construction of the plasmids for Cx43 overexpression were based on the pcDNA 3.0 vector. The rat mRNA pool, which was extracted from rat astrocyte primary cultures, was utilized to amplify sequences for Cx43 expression. Then, the fragments were inserted into the pcDNA 3.0 vector. The sequence-verified vector for Cx43 overexpression was transfected into astrocytes via an AMAXA Nucleofector kit (Lonza, CAT# VPG-1003, VPG-1006) following the protocols provided by the manufacturers.

Cx43 RNAi plasmids and Ephrin-A4 RNAi plasmids were purchased from Santa Cruz Biotechnology (CAT# sc-60008-SH) and Thermo Open Biosystems (CAT# RHS4531). Both of these RNAi plasmids were transfected into astrocytes via an AMAXA Nucleofector kit following the protocols pro-

vided by the manufacturers.

Protein extraction and Western blot

The cells were lysed with RIPA buffer (Tris-HCl 50 mmol/L, pH 7.4, NaCl 150 mmol/L, EDTA 1 mmol/L, Na-deoxycholate 0.25%, NP-40 1%, PMSF 1 mmol/L, Na_3VO_4 1 mmol/L, NaF 1 mmol/L, aprotinin 10 mg/mL, leupeptin 5 mg/mL, pepstatin 5 mg/mL) for whole cell protein extraction. The separation of the membrane protein, cytoplasmic protein and nuclear protein was executed with a plasma-membrane protein extraction kit (Beyotime, CAT# P0033) and plasma-nucleus protein extraction kit (Beyotime, CAT# P0027) according to the protocols of the manufacturer.

Protein concentrations were determined with a BCA protein assay kit (Thermo Fisher Scientific, CAT# 23227) based on the protocols of the manufacturer. Then, protein samples were loaded and ran on 10% or 12% denatured polyacrylamide gels. After protein samples of a certain molecular weight were separated via electrophoresis, the samples that remained on the gel were transferred onto a PVDF membrane (0.25 or 0.45 μm, Millipore) usingthe Bio-Rad wet transfer system. Blocking of non-specific protein binding sites in the PVDF membrane for 1 h at room temperature was performed with 5% non-fat milk powder and 5% goat serum dissolved in PBS. Then, primary antibodies were incubated in blocking buffer overnight after the antibodies were diluted: rabbit anti-Connexin 43 (CST, CAT# 3512, 1:1000), rabbit anti-Ephrin-A4 (Santa Cruz Biotechnology, CAT# sc914, 1:300), rabbit anti-CREB (CST, CAT# 4820, 1:1000), mouse anti-TFIIB (CST, CAT# 4169, 1:1000), and rabbit anti-β-Actin (Abmart, CAT# P30002, 1:1500). The PVDF membranes with protein samples were incubated with anti-rabbit or anti-mouse horseradish peroxidase conjugated secondary antibodies for 1 h at room temperature after the primary antibodies were washed with TBST buffer. An ECL kit (ThermoFisher Scientific, CAT# 34080) was subsequently utilized to detect the samples.

Immunocytochemistry and immunohistochemistry staining

The cells were fixed with 4% polyformaldehyde and perforated with 0.1% Triton X-100. The cells were then washed with PBS for three times, and the perforated samples were blocked with PBS/5% goat or donkey serum/5% BSA for 1 h at room temperature. Primary antibody incubation was performed at 2–8 °C overnight and was then followed by secondary antibody (Alexa Fluor 555 goat anti-rabbit IgG CAT# A21428, Alexa Fluor 488 goat anti-rabbit IgG CAT# A11008, Alexa Fluor 555 goat anti-Mouse IgG CAT# A21422) incubation after being washed by PBS three times. Finally, the samples were mounted on glass slides with DAKO mounting reagent (CAT# S3023).

Wheat germ agglutinin-Alexa Fluor488 (Invitrogen, CAT# W11261) was added into the cell cultures at a concentration of 5.0 μg/mL, and this incubation was maintained for 5 min if the cell membrane was to be stained. Then, fixation with 4% polyformaldehyde was performed.

Brain tissues were dehydrated with 30% sucrose solution after being fixed with 4% formaldehyde, and then, brain slices were obtained via frozen section with a Leica freezing microtome. The perforation, blocking and antibody incubations were performed identically for each treatment of the cell samples.

The cell nuclei were stained with 4′,6-diamidine-2′-phenylindole dihydrochloride (DAPI, Roche Diagnostics, CAT# 10236276001) at a concentration of 100 ng/mL.

Dilution of the antibodies was performed for rabbit anti-Connexin 43(CST, 1:100), mouse anti-GFAP (Millipore, 1:300), mouse anti-β-TubulinIII (CST, CAT# 5666), rabbit anti-Ephrin-A4 (Santa Cruz Biotechnology, 1:25), rabbit anti-EphA4 (Abcam, CAT# ab5396, 1:100), mouse anti-NSE (Millipore, CAT# MAB314, 1:10), and Alexa fluorescent dye-conjugated secondary antibodies (1:300).

Confocal microscopy

All the fluorescent staining samples were imaged with an Olympus FV 1000 laser scanning confocal microscope. The Cx43 distributions in astrocytes and the cortical neurons cultured with astrocytes were observed with a 40×0.95 numerical aperture objective lens. The brain slices was observed with a 10×0.4 and 20×0.75 objective lens.

Determination of intracellular calcium concentrations

Primary cultures of astrocytes were plated in 96-well plates. After 48 h, the cultures of astrocytes were treated with OGD/R and then washed with D-Hanks buffer. Fluo-4 AM (5 μmol/L, with 1% pluronic F-127) loading proceeded in D-Hanks (30 min, 37 °C). After washing with D-Hanks, the fluorescent astrocytes were detected (λ_{ex}=485 nm, λ_{em}=520 nm) with a NOVO star cell-based fast kinetic microplate reader (BMG, Germany). The relative concentration of cytoplasmic calcium was calculated as $[Ca^{2+}]_r$ $(F-F_{min})/(F_{max}-F)$ (F_{max}: fluorescent intensity after the cells were perforated with 1% Triton X-100; F_{min}: fluorescent intensity after calcium was chelated with 10 mmol/L EDTA.)

Chromatin immunoprecipitation

All the procedures followed the protocol in the manual from the Abcam ChIP kit (Abcam, CAT# ab500). Briefly, the nuclear content of the astrocytes was extracted, and the chromatin was sonicated into fragments. Chromatin fragments bound with CREB were pulled down by CREB antibodies. After the decrosslinking between DNA fragments of chromatin and CREB, the amount of fragments pulled down by CREB antibodies were detected with semi-quantitative PCR.

The following primer sequences were used: forward 5′-ATGCGGCTGTTGCCCCTGCTGCGGACTGTG-3′ and reverse 5′-GTTAGTGGAGTTCCAGTAGATAGAGTGGCG-3′.

Real-time polymerase chain reaction

Total RNA was extracted with TRIzol reagent (Invitrogen, CAT# USA15596018) and then precipitated with isopropanol. The reverse transcription and real-time PCR kits were purchased from TAKARA. Real-time PCR were carried out with

an ABI 7500 Fast real-time PCR system.

Primers sequences were as follows: Connexin 43 forward 5′-GGATTGAAGAGCACGGCAAGG-3′, Connexin 43 reverse 5′-ACCACTGGATGAGCAGGAAGG-3′, Ephrin-A4 forward 5′-ATGCGGCTGTTGCCCCTGC-3′, Ephrin-A4 reverse 5′-AGATGTCTAGGTAATCGTTG-3′, β-Actin forward 5′-TATGAGGGTTACGCGCTCCC-3′ and β-Actin reverse 5′-ACGCTCGGTCAGGATCTTCA-3′.

Statistical analysis

All the data were analyzed with one-way ANOVA followed by Dunnett's *post hoc* comparison or Student's *t*-test using GraphPad Prism 5 software. Error bars in each bar chart represent ±SEM.

Results

Cx43 in astrocytes underwent dynamic variation during OGD/R

Cx43 is necessary for maintaining the normal function of astrocytes by being anchored in the cytoplasmic membrane. Cx43 in astrocytes was mainly distributed in the plasma membrane, particularly adjacent to two cells (Figure 1A). While in the cytoplasm, Cx43 was also located in cellular organelles (which might be the Golgi apparatus and endoplasmic reticulum for the synthesis of lysosomes for regular degradation) around the nucleus. We utilized OGD/R to simulate hypoxia and nutritional deficiency generated by an ischemic stroke. Purified astrocytes were treated with OGD for 6 h and then reperfused. It was found that the adhesion between two adjacent cells was damaged, and the cells were retracted (Figure 1B and 1E). The total protein of Cx43 was also reduced after OGD/R (Figure 1C and 1D). The Cx43 located in the plasma membrane was distributed in the cytoplasm and accompanied by cell retraction during OGD/R (Figure 1B and 1E). We found that Cx43 was translocated from the cell membrane to the cytoplasm at the beginning of recovery after OGD. We separated the cytoplasm and membrane protein fractions of the astrocytes and

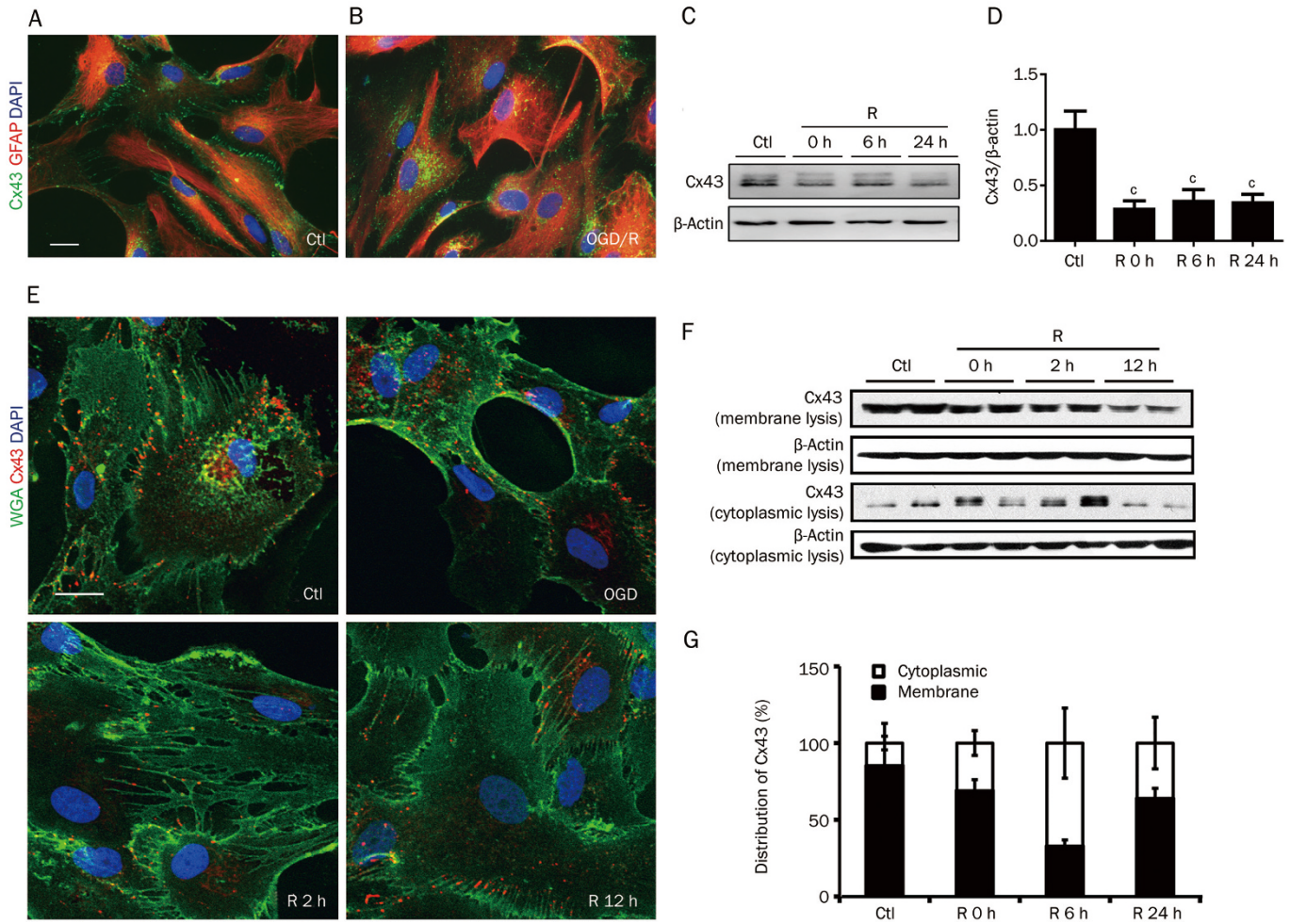

Figure 1. The dynamic distribution of Cx43. (A) Under normal circumstances, Cx43 is anchored in the plasma membrane; (B) After OGD/R, Cx43 accumulated around the nucleus. (C and D) Western blot analysis of Cx43 from the whole cell lysates of astrocyte. The dynamic Cx43 distribution and quantity were detected via immunofluorescent staining (E) and Western blot (F), respectively. The ratio of membrane Cx43 versus cytoplasmic Cx43 was calculated (G). Scale bar: A=20 μm, E=10 μm. n=3. ^{c}P<0.01 compared with the control group (one-way ANOVA followed by Dunnett's *post hoc* comparison). R: reperfution; WGA: wheat germ agglutinin.

then performed a Western blot assay with the anti-Cx43 antibody. The results showed that the protein level of the Cx43 membrane fraction was decreased after OGD. The cytoplasm fraction increased, although the restoration of membrane-anchored Cx43 also progressed (Figure 1F and 1G). Moreover, during the recovery, the recovery of adhesion astrocytes was correlated with the restoration of Cx43 anchored in the cell membrane. Overexpressed Cx43 in astrocytes could alleviate the retraction caused by OGD. It could be observed that Cx43 was still anchored in the plasma membrane where two cells were adjoined (Figure 2A and 2B). This indicated that Cx43 may play a role in sustaining cell-cell adhesion in OGD/R.

The upregulated expression of Ephrin-A4 caused by OGD/R

It is well known that astrocytes are activated after brain injury, such as ischemic stroke. The astrocytes amplify neuroinflammation by secreting various types of cytokines and chemokines. Meanwhile, they can proliferate to form glial scars. The glial scar embodies the extracellular matrix and includes a plethora of components to impede the growth of neurons, such as chondroitin sulfate proteoglycans, Sema3A, fibronectin, and collagen[3, 4]. Next, we wanted to know whether the

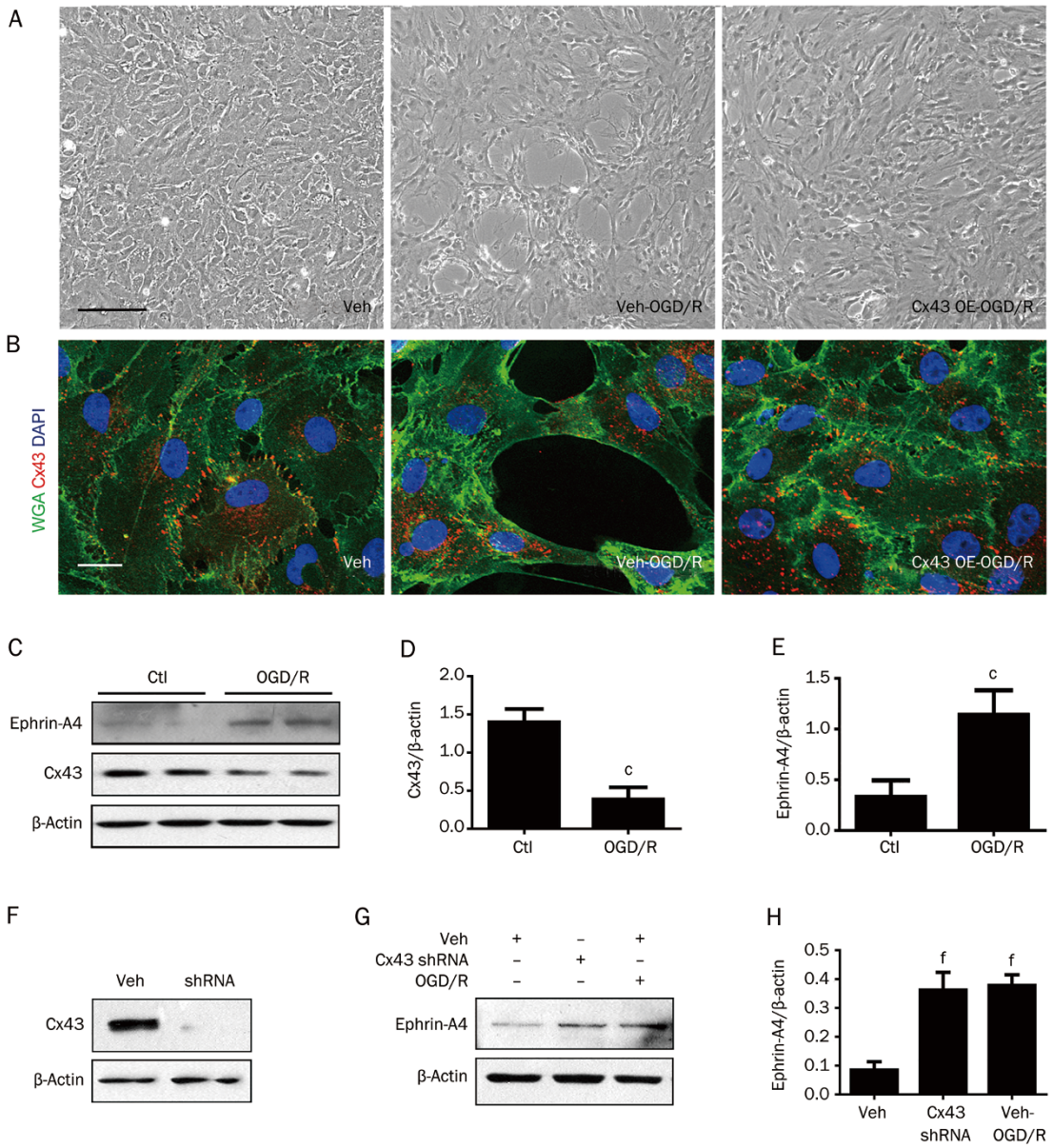

Figure 2. Degradation of Cx43 is indispensable for the upregulation of Ephrin-A4 in astrocytes treated with OGD/R. Overexpression of Cx43 (Cx43 OE) could attenuate the cell retraction caused by OGD. The results of phase contrast (A) and confocal microscopy (B); OGD/R incurred degradation of Cx43 brought about the upregulation of Ephrin-A4 (C–E); shRNA plasmid targeting Cx43 could efficiently knockdown the Cx43 protein level (F); the knockdown of Cx43 could also upregulate Ephrin-A4 expression levels (G, H). Scale bar: A=10 μm, B=10 μm. n=4. ^{c}P<0.01 compared with the control. ^{f}P<0.01 compared with the vehicle (one-way ANOVA followed by Dunnett's *post hoc* comparison). WGA: wheat germ agglutinin; Veh: vehicle; R: reperfusion.

decrease in Cx43 after OGD/R had any effect on Ephrin-A4. We investigated the changes in Ephrin-A4 on astrocytes after OGD/R. First, we detected the expression of Ephrin-A4 with a Western blot assay. The results showed that the expression of Ephrin-A4 was upregulated after OGD/R (Figure 2C). We found that the upregulation of Ephrin-A4 was consistent with the downregulation of Cx43 (Figure 2D and 2E). To confirm these results, we knocked down the expression of Cx43 in astrocytes with RNAi, and the results of a Western blot assay showed that the expression of Ephrin-A4 was also significantly increased after OGD/R (Figure 2F, 2G, and 2H).

The upregulated expression of Ephrin-A4 was mediated through the CaMKII/CREB pathway

Many studies have revealed that various physiological and pathological activities of astrocytes were closely associated with calcium. As glial cells are predominant in the central nervous system, astrocytes function as colossal calcium reservoirs[16]. Numerous factors (agonists of Gq GPCR, ATP, and mechanical stumili) could trigger a calcium influx[17–19]. The pathological extracellular concentration of potassium induces the uptake of calcium into the astrocytes, and to some extent, the extracellular calcium could be scavenged to alleviate the possibility of neuronal calcium overloading[20, 21]. On all counts, the astrocytes contributed to the homeostasis of calcium. Transmission of calcium waves is a direct way for astrocytes to convey information[22, 23]. The functional syncytium based on gap junctions between astrocytes allows the transmission of excitation with rapidity and efficiency.

To determine the underlying cellular and molecular mechanisms for the increase in Ephrin-A4, we postulated that after treatment with OGD/R, the dislocation and following degradation of Cx43 in astrocytes could possibly disturb the homeostasis of intracellular calcium and subsequently initiate the calcium-related signaling pathway for the translation of Ephrin-A4. Then, we assessed the concentration of the intercellular calcium with fluo-4 AM loading. The results showed that intercellular calcium was significantly increased after OGD/R (Figure 3A). Overexpression of Cx43 could attenuate upregulation of the calcium concentration induced by OGD/R. Knockdown of Cx43 expression with RNAi increased the concentration of calcium in astrocytes (Figure 3A). EGTA is a calcium chelator, and by using EGTA to chelate the calcium in the culture system, the increase in cytoplasmic calcium concentrations and the upregulation of Ephrin-A4 after OGD/R was alleviated (Figure 3B and 3C), indicating the significance of calcium overloading for the upregulation of Ephrin-A4. It was reported that the expression of Ephrin-A4 was more likely mediated by the CaMKII/CREB signaling pathway[24]. Then, we determined the translocation of CREB into the nucleus. We found that the translocation of CREB was obviously increased in astrocytes after OGD/R. The administration of KN-93, an

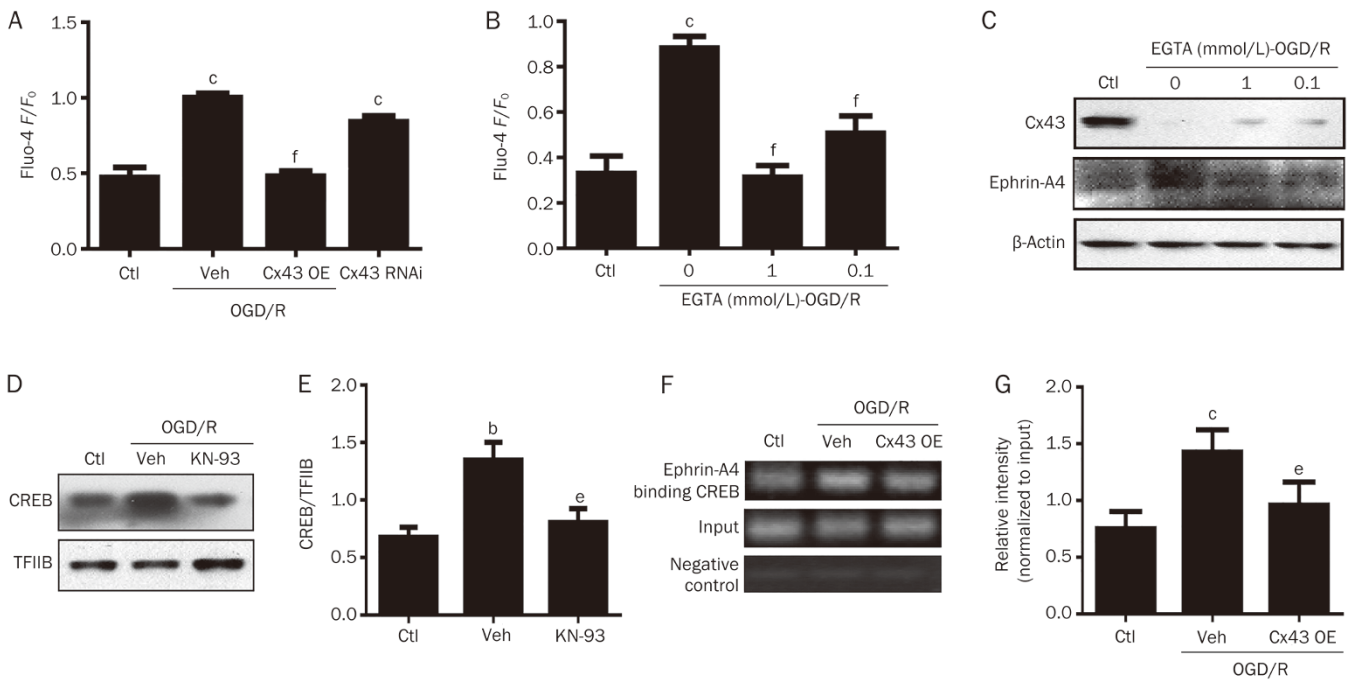

Figure 3. OGD/R upregulated the expression of Ephrin-A4 by raising the calcium level. (A) Increased cytoplasmic calcium concentration is a downstream event of OGD/R incurring Cx43 degradation; (B) EGTA could block the elevated calcium concentration caused by OGD/R; (C) EGTA could inhibit the upregulation of Ephrin-A4 in astrocytes treated with OGD/R; (D and E) KN-93 could reverse the enhanced translocation of CREB into the nucleus caused by OGD/R; (F and G) Overexpression of Cx43 could lessen the binding of CREB with DNA sequencing of the gene encoding Ephrin-A4 in the chromatin. $^{b}P<0.05$, $^{c}P<0.01$ compared with control group. $n=3$. $^{e}P<0.05$, $^{f}P<0.01$ compared with the OGD/R group (one-way ANOVA followed by Dunnett's *post hoc* comparison). Veh: vehicle; R: reperfusion; OE: overexpression.

inhibitor of CaMKII, could reverse the enhancement of CREB nuclear translocation caused by OGD/R, indicating that the incremental CREB in the nucleus was mainly mediated by the activation of CaMKII (Figure 3D and 3E). Next, we detected the amount of CREB binding the chromatin partition of the DNA sequence of the gene encoding Ephrin-A4 via chromatin immunoprecipitation (ChIP). It showed that the amount of Ephrin-A4 binding CREB was enhanced after treatment with OGD/R (Figure 3F and 3G). Overexpression of Cx43 abated the increased CREB in the nucleus and lessened the binding of CREB by DNA sequencing the gene encoding Ephrin-A4 in chromatin (Figure 3F and 3G), solidifying the role of Cx43 in inhibiting the upregulation of Ephrin-A4 expression caused by OGD/R.

The maintenance of Cx43 in the membranes of astrocytes was indispensable to neuronal growth

It has been reported that Ephrin-A4 could inhibit neurite growth in dorsal root ganglion cells[5]. For astrocytes, the activation of EphA4 leads to astrogliosis, but for neurons, it inhibits the growth of neurites[25]. We used neuron specific enolase (NSE) to mark neurons. We confirmed that EphA4 (the receptor of Ephrin-A4) was expressed in the cortical neurons plated on astrocytes (Figure 4A). Additionally, it was found that the protein expression of Ephrin-A4 was upregulated after treatment with OGD/R, and shRNA plasmid targeting Ephrin-A4 could knockdown Ephrin-A4 in astrocytes treated with OGD/R (Figure 4B). Numerous studies have revealed that astrocytes could be activated[26–28], in which state they would

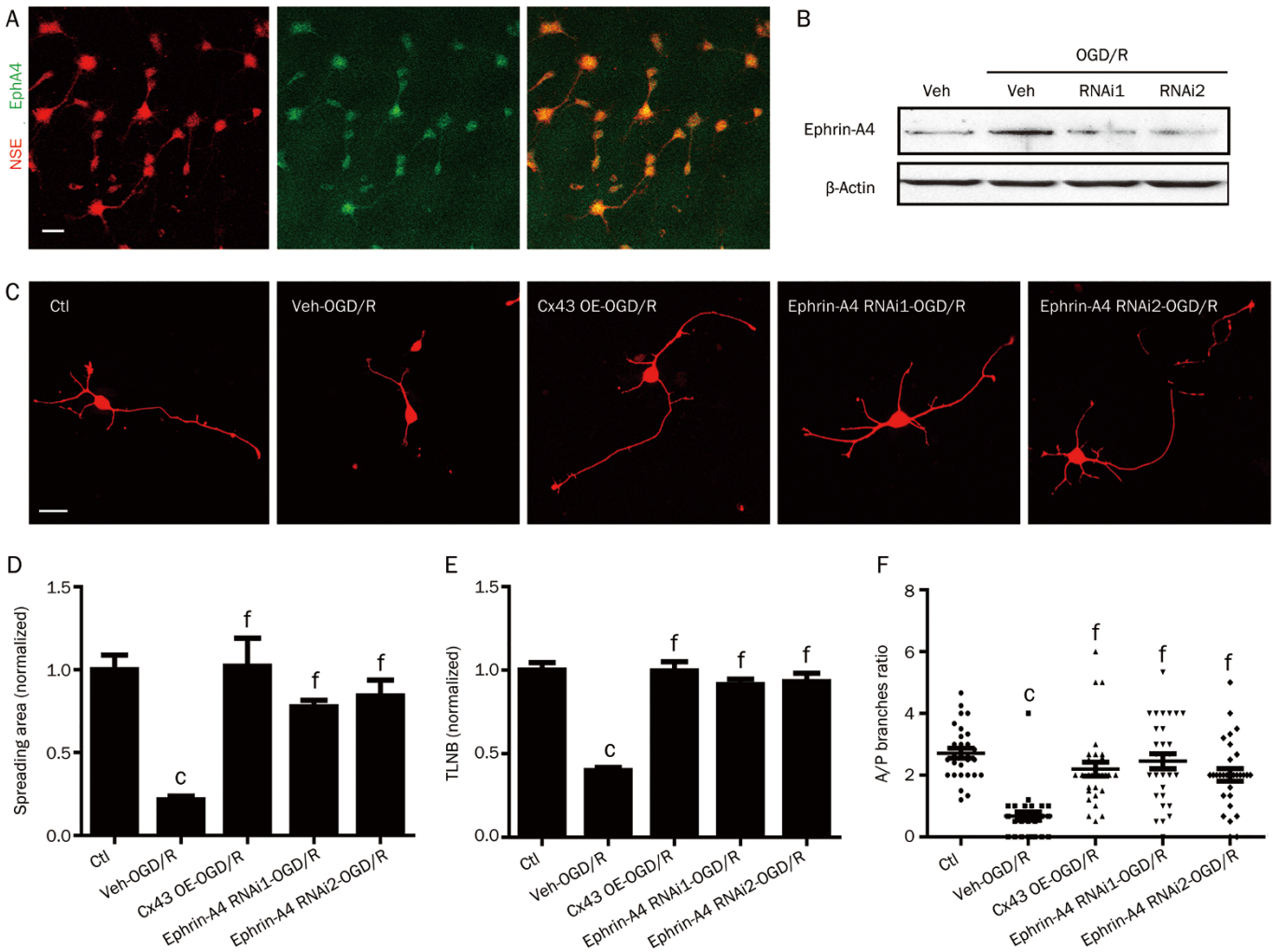

Figure 4. Neurons cultured on astrocytes treated with OGD/R grew with a retarded status. (A) The cortical neurons plated on astrocytes expressed EphA4; (B) RNAi1 and RNAi2, two types of shRNA plasmid with different targeting sequences for Ephrin-A4, could knockdown Ephrin-A4 in astrocytes treated with OGD/R; (C) Cortical neurons were inadaptable to astrocytes treated with OGD/R (2nd block), and the overexpression of Cx43 in astrocytes could reverse the hostile status of astrocytes (3rd block); RNAi of Ephrin-A4 led to the malnourished growth of neurons (4th and 5th blocks); (D–F) Spreading area, shortened total length of neurite branches (TLNB) and low advanced/primary branch (A/P) ratios were calculated. Scale bar: A=20 μm, C=10 μm. n=20. ^{c}P<0.01 compared with the control group; ^{f}P<0.01 compared with the OGD/R group (one-way ANOVA followed by Dunnett's *post hoc* comparison).

hamper neuronal recovery in stroke and neurodegenerative disorders. To promote brain recovery from disorders such as a stroke, the function of astrocytes should be restored. Cx43 plays a very important role in maintaining the integrity of the astrocyte membrane and astrocyte function. We analyzed the mechanism for this using a co-culture of astrocytes and neurons. The primary culture of cortical neurons were plated on astrocytes treated with or without OGD/R. The length of neurites and branches spreading to neuronal areas are illustrated. It was observed that the neurons cultured on astrocytes with OGD/R had shortened total lengths of neurite branches (TLNBs) and low advanced/primary branch (A/P) ratios compared to the control groups (Figure 4C–4F). Because maintaining a sufficient amount of Cx43 could ameliorate cell retraction and stabilize astrocytes, we overexpressed Cx43 in astrocytes. The results showed that the cortical neurons cultured with astrocytes treated with OGD/R were also rescued by the overexpression of Cx43 and were prone to grow better (Figure 4C–4F). According to these outcomes, it is rational to postulate that the overexpression of Cx43 can attenuate the upregulation of Ephin-A4 in astrocytes treated with OGD/R and facilitate neuronal growth. Therefore, the maintenance of Cx43 in the membranes of astrocytes was crucial to neuronal growth.

Neuronal recovery correlated with the recuperation of Cx43 and Ephrin-A4 in astrocytes

To investigate whether neuronal recovery was correlated with the recuperation of Cx43 and Ephrin-A4 in astrocytes, we utilized MCAO model rats. As a single side of MCAO could generate an infarct in a certain brain area (Figure 5A), we observed changes in Cx43 and Ephrin-A4 in astrocytes adjacent to the infarct area and during neuronal recovery. One side of the model rat brain underwent ischemia for 1 h, and then, the blood supply was recovered by reperfusion. After 24 h of reperfusion, the infarct area could be observed with an obvious boundary by GFAP staining (Figure 5B). The astrocytes in the area adjacent to the infarct zone revealed a lack of β-Tubulin III and GFAP staining compared to that of the intact area far from the infarct zone. Moreover, the distribution of astrocytes was closer to the infarct area than that of neurons. It seemed that astrocytes demarcated the zone for neuronal growth (Figure 5B). However, GFAP and β-Tubulin III staining could be observed in the contralateral area corresponding to the ipsilateral infarct area (Supplementary Figure 1A). After eight days of recovery, the neuronal staining was located in the area that was supposed to be the infarct zone but was still lacking astrocyte staining, indicating a disruption in neuronal growth through the demarcation of astrocytes to the infarct area (Figure 6A), while the distribution of neuronal and astroglial staining in the contralateral areas were still similar to seven days before (Supplementary Figure 1B). Furthermore, the staining of Cx43 and Ephrin-A4 in astrocytes of the area surrounding the infarct area had as much intensity as astrocytes of the contralateral brain (Figures 6B and 6C). In other words, neuronal growth was initiated when Cx43 and

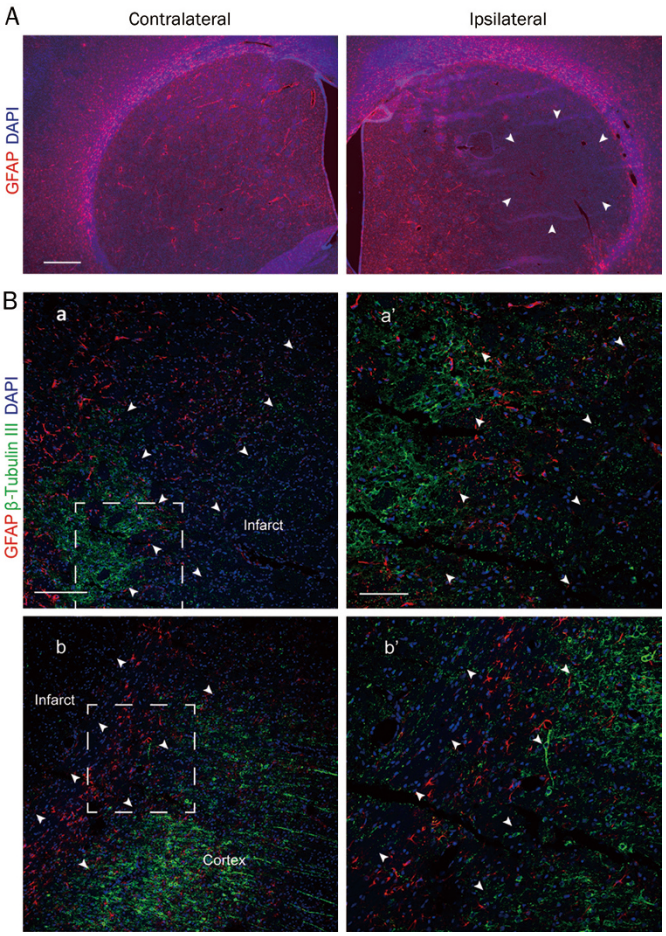

Figure 5. Astrocytes in the ipsilateral brain area of the MCAO bordered infarct area after 24 h ischemia. (A) A single side of the MCAO could generate an infarct of a certain brain area (defined by arrows); (B) a and a′: the striatum near the lateral ventricle; b and b′: the cortex-corpus callosum-striatum. a′ and b′ are magnified images of a and b, respectively (the magnified area in a and b are marked with broken line squares). Arrows illustrate the border of β-Tubulin III staining adjacent to the relatively intact area and the border of GFAP staining adjacent to the infarct area. Scale bar: A=500 μm, a, b=200 μm. a′, b′=100 μm.

Ephrin-A4 in astrocytes surrounding the infarct area recovered to normal states.

Bederson's neurological scoring scale was utilized to evaluate the behavioral dysfunction caused by MCAO: 0=no obvious behavioral changes, 1=contralateral forelimb bends after the rat is suspended, 2=lowered repelling forces of the contralateral limbs, 3=swirling to the damaged side after tail hung, but during free ambulation, no observable swirling, and 4=spontaneous swirling to the damaged side. It was found that neurological scores after seven days of reperfusion were significantly lower than that of one day of reperfusion (2.40±0.24 *vs* 3.00±0.00, $^{b}P<0.05$), indicating the recuperation of rats with MCAO treatment after seven days of reperfusion. These results were consistent with the neuronal recovery verified by immunofluorescent staining (Supplementary Figure 2).

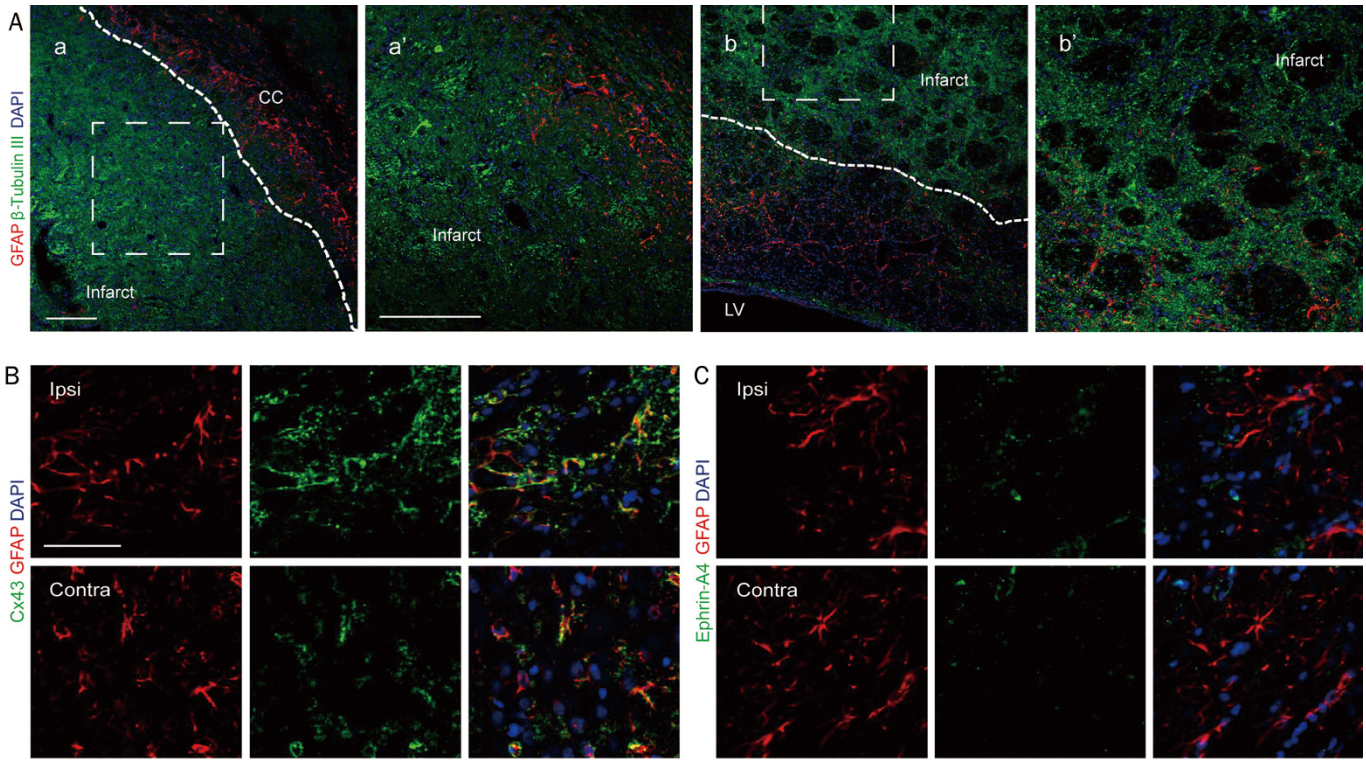

Figure 6. Positive staining of β-Tubulin III reappeared in the infarct brain area after eight days of reperfusion. (A) a and a′: the cortex-corpus callosum (CC)-striatum. b and b′: the striatum near to the lateral ventricle. Broken lines illustrate the border adjacent to the infarct area; a′ and b′ are magnified images of a and b, respectively (the magnified area in a and b were marked with broken line squares). (B) The expression of Cx43 was recovered after eight days of reperfusion. (C) The expression of Ephrin-A4 was recovered to a normal state. Scale bar: A=200 μm, B=50 μm.

Discussion

Astrocytes make up approximately 40%±50% of all glial cells and play important roles in brain homeostasis. Cx43, which is mainly expressed in the astrocytes of the CNS, is a member of the connexin family, comprising two types of functional units, gap junctions and hemichannels. The gap junction is undoubtedly an important structure for astrocytes to maintain brain homeostasis. Cx43 shows a strong ability to maintain the normal shape and function of astrocytes. The dynamic distribution of Cx43, consisting of the transport of Cx43 into the cytoplasmic membrane and internalization of Cx43, takes place by regular turnover[29] and in abnormal states of the cells[30–32]. The alterations in the dynamic distribution of Cx43 in cells undergoing morbidity could be normal in certain roles. Stroke or brain ischemia comprises miscellaneous factors that could generate abnormal changes in Cx43. However, links are still missing regarding the pathological factors and changes in Cx43.

Our results showed that OGD/R could alter the location of Cx43 in astrocytes and induce an increase in Ephrin-A4. The latter is a nerve growth inhibitory factor. Interestingly, the activation of EphA4 could also potentially trigger astrogliosis[33, 34]. To summarizethese outcomes, the dislocation and degradation of Cx43, activation of EphA4 and astrogliosis probably comprise a feed-forward cycle, which could be initiated by a stroke-like milieu with the dislocation of Cx43. Then, the ongoing nature of this vicious cycle alters homeostasis in astrocytes and disturbs the balance of neuron-glia. Therefore, ensuring sufficient Cx43 in the plasma membrane could "extinguish the fire before it flares." It is likely that Cx43 could be a defender of or gate in the plasma membrane of astrocytes. If they were dislocated or destroyed, astrocytes would undergo what occurs in a stroke-like milieu.

Cx43 and its related functional units maintain cell integrity and cell-cell communication, which would mediate the protective effect of astrocytes in hypoxic preconditioning[35]. A milieu of neuroinflammation and metabolic inhibition could disturb the aforementioned function of Cx43 in astrocytes under normal conditions[36, 37]. We postulated that Cx43 could maintain homeostasis in cells; thus, the degradation of Cx43 caused by OGD/R could disturb cell communication and substance exchanges, leading to the disruption of homeostasis. A viewpoint has been offered that neuroprotection should be equal for the protection of neurons and astrocytes. The protection of astrocytes could not only facilitate the preservation of the integrity of brain matter but also be beneficial for the growth of neurons. Heretofore, there have been few studies associated with the relationship between Cx43 in astrocytes and the growth of neurons. It was previously reported that Cx43-mediated calcium waves could guide axon growth

directly[38]. Maintaining the distribution of Cx43 in the plasma membrane has its own advantages for therapy in strokes. Cells are maintained by Cx43 in their normal states by modulating the activities of certain pathways rather than purely suppressing them. Hence, the associated adverse effect could be avoided. Additionally, this strategy does not focus on certain types of pathways to compensate for deleterious responses generated by stroke. Instead, the stabilization exerted by Cx43 could diminish abnormal changes upstream, which is possibly more efficient and lucrative.

It is crucial to avoid the "trigger one, run all" dilemma in the complex of cellular signaling pathways by stabilizing astrocytes rather than inhibiting the activity of the signal inflammatory pathway. Coalescence of neuron-death-prevention and neuron-recovery promotion might be a silver lining for the gloomy cloak of stroke, which would rationalize the potentiality of Cx43 as a target for the therapy of stroke based on astrocytes.

Acknowledgements

This work was supported by grants from the National Natural Science Foundation of China (81123004), the Scientific Innovation Project of the Chinese Academy of Sciences (XDA 01040304) and National Science & Technology Major Project "Key New Drug Creation and Manufacturing Program" (2014ZX09102-001-05).

Author contribution

Lin-yin FENG conceived and designed the experiments; Le-yu WU and Xue-li YU performed experiments and analyzed the data; Le-yu WU and Lin-yin FENG wrote the manuscript.

Supplementary information

Supplementary information is available at Acta Pharmacologica Sinica's website.

References

1 O'Collins VE, Macleod MR, Donnan GA, Horky LL, van der Worp BH, Howells DW. 1026 experimental treatments in acute stroke. Ann Neurol 2006; 59: 467–77.
2 Verkhratsky A, Parpura V. Recent advances in (patho)physiology of astroglia. Acta Pharmacol Sin 2010; 31: 1044–54.
3 Nieto-Sampedro M. Neurite outgrowth inhibitors in gliotic tissue. Adv Exp Med Biol 1999; 468: 207–24.
4 Pasterkamp RJ, Anderson PN, Verhaagen J. Peripheral nerve injury fails to induce growth of lesioned ascending dorsal column axons into spinal cord scar tissue expressing the axon repellent Semaphorin 3A. Eur J Neurosci 2001; 13: 457–71.
5 Moss A, Alvares D, Meredith-Middleton J, Robinson M, Slater R, Hunt SP, *et al*. Ephrin-A4 inhibits sensory neurite outgrowth and is regulated by neonatal skin wounding. Eur J Neurosci 2005; 22: 2413–21.
6 Han Y, Yu HX, Sun ML, Wang Y, Xi W, Yu YQ. Astrocyte-restricted disruption of connexin-43 impairs neuronal plasticity in mouse barrel cortex. Eur J Neurosci 2014; 39: 35–45.
7 Retamal MA, Froger N, Palacios-Prado N, Ezan P, Saez PJ, Saez JC, *et al*. Cx43 hemichannels and gap junction channels in astrocytes are regulated oppositely by proinflammatory cytokines released from activated microglia. J Neurosci 2007; 27: 13781–92.
8 Rouach N, Calvo CF, Glowinski J, Giaume C. Brain macrophages inhibit gap junctional communication and downregulate connexin 43 expression in cultured astrocytes. Eur J Neurosci 2002; 15: 403–7.
9 Meme W, Calvo CF, Froger N, Ezan P, Amigou E, Koulakoff A, *et al*. Proinflammatory cytokines released from microglia inhibit gap junctions in astrocytes: potentiation by beta-amyloid. FASEB J 2006; 20: 494–6.
10 Orellana JA, Hernandez DE, Ezan P, Velarde V, Bennett MV, Giaume C, *et al*. Hypoxia in high glucose followed by reoxygenation in normal glucose reduces the viability of cortical astrocytes through increased permeability of connexin 43 hemichannels. Glia 2010; 58: 329–43.
11 Nakase T, Fushiki S, Naus CC. Astrocytic gap junctions composed of connexin 43 reduce apoptotic neuronal damage in cerebral ischemia. Stroke 2003; 34: 1987–93.
12 Gao Q, Katakowski M, Chen X, Li Y, Chopp M. Human marrow stromal cells enhance connexin 43 gap junction intercellular communication in cultured astrocytes. Cell Transplant 2005; 14: 109–17.
13 Zhang C, Li Y, Chen J, Gao Q, Zacharek A, Kapke A, *et al*. Bone marrow stromal cells upregulate expression of bone morphogenetic proteins 2 and 4, gap junction protein connexin-43 and synaptophysin after stroke in rats. Neuroscience 2006; 141: 687–95.
14 Hoehn BD, Palmer TD, Steinberg GK. Neurogenesis in rats after focal cerebral ischemia is enhanced by indomethacin. Stroke 2005; 36: 2718–24.
15 Zheng YQ, Liu JX, Li XZ, Xu L, Xu YG. RNA interference-mediated downregulation of Beclin1 attenuates cerebral ischemic injury in rats. Acta Pharmacol Sin 2009; 30: 919–27.
16 Gambetti P, Erulkar SE, Somlyo AP, Gonatas NK. Calcium-containing structures in vertebrate glial cells. Ultrastructural and microprobe analysis. J Cell Biol 1975; 64: 322–30.
17 Barres BA, Chun LL, Corey DP. Calcium current in cortical astrocytes: induction by cAMP and neurotransmitters and permissive effect of serum factors. J Neurosci 1989; 9: 3169–75.
18 Cornell-Bell AH, Finkbeiner SM, Cooper MS, Smith SJ. Glutamate induces calcium waves in cultured astrocytes: long-range glial signaling. Science 1990; 247: 470–3.
19 Neary JT, van Breemen C, Forster E, Norenberg LO, Norenberg MD. ATP stimulates calcium influx in primary astrocyte cultures. Biochem Biophys Res Commun 1988; 157: 1410–6.
20 Duffy S, MacVicar BA. *In vitro* ischemia promotes calcium influx and intracellular calcium release in hippocampal astrocytes. J Neurosci 1996; 16: 71–81.
21 Hertz L, Bender AS, Woodbury DM, White HS. Potassium-stimulated calcium uptake in astrocytes and its potent inhibition by nimodipine. J Neurosci Res 1989; 22: 209–15.
22 Fellin T, Pascual O, Gobbo S, Pozzan T, Haydon PG, Carmignoto G. Neuronal synchrony mediated by astrocytic glutamate through activation of extrasynaptic NMDA receptors. Neuron 2004; 43: 729–43.
23 Panatier A, Vallee J, Haber M, Murai KK, Lacaille JC, Robitaille R. Astrocytes are endogenous regulators of basal transmission at central synapses. Cell 2011; 146: 785–98.
24 Akaneya Y, Sohya K, Kitamura A, Kimura F, Washburn C, Zhou R, *et al*. Ephrin-A5 and EphA5 interaction induces synaptogenesis during early hippocampal development. PLoS One 2010; 5: e12486.
25 Goldshmit Y, Galea MP, Wise G, Bartlett PF, Turnley AM. Axonal regeneration and lack of astrocytic gliosis in EphA4-deficient mice. J Neurosci 2004; 24: 10064–73.
26 McKeon RJ, Jurynec MJ, Buck CR. The chondroitin sulfate proteoglycans neurocan and phosphacan are expressed by reactive astro-

cytes in the chronic CNS glial scar. J Neurosci 1999; 19: 10778–88.
27 Jones LL, Margolis RU, Tuszynski MH. The chondroitin sulfate proteoglycans neurocan, brevican, phosphacan, and versican are differentially regulated following spinal cord injury. Exp Neurol 2003; 182: 399–411.
28 Wu DD, Huang L, Zhang L, Wu LY, Li YC, Feng L. LLDT-67 attenuates MPTP-induced neurotoxicity in mice by up-regulating NGF expression. Acta Pharmacol Sin 2012; 33: 1187–94.
29 Nickel BM, DeFranco BH, Gay VL, Murray SA. Clathrin and Cx43 gap junction plaque endoexocytosis. Biochem Biophys Res Commun 2008; 374: 679–82.
30 Gilleron J, Fiorini C, Carette D, Avondet C, Falk MM, Segretain D, *et al*. Molecular reorganization of Cx43, Zo-1 and Src complexes during the endocytosis of gap junction plaques in response to a non-genomic carcinogen. J Cell Sci 2008; 121: 4069–78.
31 Danon A, Zeevi-Levin N, Pinkovich DY, Michaeli T, Berkovich A, Flugelman M, *et al*. Hypoxia causes connexin 43 internalization in neonatal rat ventricular myocytes. Gen Physiol Biophys 2010; 29: 222–33.
32 Zhang GL, Yu F, Dai DZ, Cheng YS, Zhang C, Dai Y. CPU86017-RS attenuate hypoxia-induced testicular dysfunction in mice by normalizing androgen biosynthesis genes and pro-inflammatory cytokines. Acta Pharmacol Sin 2012; 33: 470–8.
33 Parmentier-Batteur S, Finger EN, Krishnan R, Rajapakse HA, Sanders JM, Kandpal G, *et al*. Attenuation of scratch-induced reactive astrogliosis by novel EphA4 kinase inhibitors. J Neurochem 2011; 118: 1016–31.
34 Goldshmit Y, Bourne J. Upregulation of EphA4 on astrocytes potentially mediates astrocytic gliosis after cortical lesion in the marmoset monkey. J Neurotrauma 2010; 27: 1321–32.
35 Lin JH, Lou N, Kang N, Takano T, Hu F, Han X, *et al*. A central role of connexin 43 in hypoxic preconditioning. J Neurosci 2008; 28: 681–95.
36 Contreras JE, Sanchez HA, Eugenin EA, Speidel D, Theis M, Willecke K, *et al*. Metabolic inhibition induces opening of unapposed connexin 43 gap junction hemichannels and reduces gap junctional communication in cortical astrocytes in culture. Proc Natl Acad Sci U S A 2002; 99: 495–500.
37 Karpuk N, Burkovetskaya M, Fritz T, Angle A, Kielian T. Neuroinflammation leads to region-dependent alterations in astrocyte gap junction communication and hemichannel activity. J Neurosci 2011; 31: 414–25.
38 Hung J, Colicos MA. Astrocytic Ca(2+) waves guide CNS growth cones to remote regions of neuronal activity. PLoS One 2008; 3: e3692.